GENERATIVE MODEL AND ASSOCIATED METRIC FOR COORDINATED-MOTION TARGET GROUPS

Léo Legrand[1],[3], *Audrey Giremus*[3], *Éric Grivel*[3], *Laurent Ratton*[2] *and Bernard Joseph*[1]

Thales Systèmes Aéroportés S.A., [1]Mérignac, [2]Élancourt, FRANCE
[3]University of Bordeaux - Bordeaux INP - IMS - UMR CNRS 5218, Talence, FRANCE

ABSTRACT

In multi-object tracking, some target groups can share a coordinated motion. They can for instance form a convoy or follow a road network. In any case, the target trajectories can be modeled by using the group motion characteristics and the self-properties of the targets. For this purpose, we introduce a new model: a hierarchical random finite set (RFS). A first RFS is considered to represent the target groups. Their numbers, their compositions and their common motion characteristics are assumed to be random. Each group is itself represented as an RFS for which the target number and the target states such as the position and velocity are random. We also propose a metric to compare two hierarchical RFSs taking into account all the sources of uncertainties (the cardinality of both the groups and the targets within the groups and the unknown motion parameters).

Index Terms— Multiple targets, target groups, coordinated motions, random finite sets, metric.

1. INTRODUCTION

Multi-object systems are of great interest in a wide range of applications such as radar surveillance and computer vision. For the last two decades, they have been represented by using the random finite set (RFS) framework [1–3]. An RFS consists of a set of unordered state vectors representing the objects of interest whose number is also random. By this way, an RFS inherently integrates the uncertainty on the target cardinal. It is also convenient to gather all the measurements available in an observation RFS, taking into account false detections. Approximate multi-object Bayes filters, such as the probability hypothesis density (PHD) filter [2], the labeled multi-Bernoulli (LMB) filter [4] or the δ-generalized labeled multi-Bernoulli (δ-GLMB) filter [5], have then been proposed to estimate the posterior distribution of the multi-object RFS from the multi-observation RFS.

To evaluate the difference between two RFSs for instance when comparing the performance of different estimation algorithms, metrics have been proposed including the Hausdorff metric [6], the optimal mass transfer (OMAT) metric [7] and the optimal sub-pattern assignment (OSPA) metric [8]. The latter has the advantage of taking into account both the errors on the state estimates of the different objects and the error on the estimated number of objects in the scene. It should be noted that several variants and complementary metrics of the OSPA exist: the Hellinger-OSPA (H-OSPA) [9], the quality-based OSPA (Q-OSPA) [10], the generalized OSPA (GOSPA) [11], the C-OSPA [12], the OSPA for tracks (OSPAT) [13] [14] or the cardinalized optimal linear assignment (COLA) metric [15]. These metrics address more specific cases than the initial OSPA. For instance, the OSPAT is designed for labeled RFSs and allows the practitioner to penalize the labeling errors.

In this paper, we are interested in multi-object scenarios where some objects tend to exhibit similarities in their behaviors or can have coordinated motions so that they can be considered as a group. In [16–19], group tracking is addressed by considering the spatial proximity of multiple measurements. They can arise from an extended target which leads to more than one point measurement. Otherwise, they can be due to two or more targets evolving with a coordination in their moves. However, due to the spatial proximity hypothesis, the considered scenarios are limited. For this reason, we introduce a more generic approach in this communication.

Our purpose is to address groups of mobile targets with coordinated motions, independently from their spatial proximity. This situation often occurs in a constrained environment. This can be a road network where the vehicles follow a restricted path and avoid collisions by keeping a safe distance between them. This is also the case of targets traveling in a convoy. In these cases, taking into account the shared motion characteristics is bound to improve the overall estimation of the target kinematics. This work is dedicated to complex scenarios wherein several groups of targets evolve simultaneously in the same scene. As a first step, our contribution is to propose a model which accounts for the different sources of uncertainties including the number of groups, the number of targets within each group and their kinematics. It consists of a hierarchical RFS. The first layer of RFS focuses on the groups and determines how many of them are present in the scene and what the shared motion characteristics are between the targets belonging to a same group. Then, a bank of RFSs, one associated to each group, represents the uncertainty on the number of targets per group and also their individual behavior. Indeed, it is quite realistic to assume that a target trajectory results both from the group influence and its own maneuver capability. This new model is intended to be used as a prior in estimation algorithms. These latter are not presented here for the lack of space and will be developed in a further paper. As a second contribution, we propose a metric to compare two hierarchical RFSs which will used for instance to evaluate estimation algorithms. It takes into account the group cardinality, the cardinality of the elements inside a group and the closeness of both the common and individual motion parameters.

The paper is organized as follows: in section 2, we recall the multi-object modeling using the RFS framework and the OSPA metric. In section 3, we present our generic generative model for groups of coordinated-motion targets. We detail two specific applications. Then, the metric associated to this hierarchical RFS model is presented. Conclusions and perspectives are finally presented in section 4.

This work is part of the common research activities between Bordeaux campus and Thales (GIS Albatros).

2. MULTI-OBJECT SYSTEMS

In multi-object systems, the number of targets is unknown and can change because of the appearance or the disappearance of a target in the region of interest. By considering this cardinality as a random variable, the RFS framework naturally captures its evolution additionally to the state of the present targets. Furthermore, RFSs avoid measure/target association issues by considering the targets as a whole.

2.1. Classical model: random finite sets

A multi-object system can be conveniently represented by an RFS denoted as follows:

$$\mathbf{X} = \{\mathbf{x}_1, \mathbf{x}_2, ..., \mathbf{x}_m\}, \text{ with } m \in \mathbb{N}, \tag{1}$$

where $\mathbf{x}_i$ denotes the state of the i^{th} target. An RFS $\mathbf{X}$ is then defined by the distribution $\rho(m)$ on its random cardinality m and the distributions of the m-uplet $\mathbf{x}_1, ..., \mathbf{x}_m$ providing the cardinal is m, denoted $p_m(\mathbf{x}_1, ..., \mathbf{x}_m)$. It should be noted that exchangeability is guaranteed if $p_m(\mathbf{x}_1, ..., \mathbf{x}_m)$ is a symmetric joint distribution. To represent in an unified manner all these variabilities, Mahler [2] introduces a probabilistic descriptor, namely a finite set statistics (FISST) probability density function (PDF) denoted $f(\mathbf{X})$ on the random set $\mathbf{X}$. It is defined as follows:

$$f\left(\{\mathbf{x}_1, ..., \mathbf{x}_m\}\right) = m!\rho(m)p_m\left(\mathbf{x}_1, ..., \mathbf{x}_m\right), \tag{2}$$

which is integrated to one according to:

$$\int f(\mathbf{X})\delta\mathbf{X} = f(\emptyset) + \sum_{m=1}^{+\infty} \frac{1}{m!} \int f\left(\{\mathbf{x}_1, ..., \mathbf{x}_m\}\right) d\mathbf{x}_1 ... d\mathbf{x}_m. \tag{3}$$

Filters performing multi-target tracking enforce an approximated Bayes recursion to calculate the posterior. To study the relevance of a filter, the OSPA metric is usually used to compare the estimated set $\mathbf{X}$ to the real set.

2.2. Metric: OSPA of order p and cut-off parameter c

Initially introduced by [20] to address problems in point process theory and spatial statistics, the OSPA metric has been mainly used to evaluate the performance of multi-object tracking algorithms [21] but also to design estimation algorithms based on the minimization of this criterion such as the so-called Minimum Mean OSPA algorithm [22]. It has been also used for clustering set-valued observations [23].

The OSPA metric between two sets $\mathbf{X} = \{\mathbf{x}_1, \mathbf{x}_2, ..., \mathbf{x}_m\}$ and $\mathbf{Y} = \{\mathbf{y}_1, \mathbf{y}_2, ..., \mathbf{y}_n\}$ is defined as follows for $m \leq n$[1]:

$$d_p^{(c)}(\mathbf{X},\mathbf{Y}) = \left(\frac{1}{n}\left(\min_{\pi\in\Pi_n} \sum_{i=1}^{m} \left[d_c\left(\mathbf{x}^{(i)}, \mathbf{y}^{(\pi(i))}\right)\right]^p + c^p\,(n-m)\right)\right)^{\frac{1}{p}}, \tag{4}$$

with $c > 0$ the cut-off parameter or clamping factor, $0 < p < +\infty$ the order, Π_n the set of permutations on $\{1, 2, ..., n\}$ and $d_c(\mathbf{x}, \mathbf{y})$ the metric between two state vectors $\mathbf{x}$ and $\mathbf{y}$ defined by:

$$d_c(\mathbf{x}, \mathbf{y}) = \min\left(c, d(\mathbf{x}, \mathbf{y})\right), \tag{5}$$

where $d(\mathbf{x}, \mathbf{y})$ is typically the Euclidean metric between the vectors $\mathbf{x}$ and $\mathbf{y}$.

Given (4) and (5), the OSPA metric [8] which is a variant of the Wasserstein metric of order p [7] takes into account both the errors on the states and the cardinality.

Selecting a large value for p penalizes large metrics between elements of $\mathbf{X}$ and elements of $\mathbf{Y}$ as well as outliers. In addition, c is usually in meters. Given (5), a metric between a state $\mathbf{y}$ and a state $\mathbf{x}$ is bounded to c, *i.e.* is in $[0,\ c]$. Then, when looking at (4), the cut-off parameter c is a way to weight the cardinality error against the localization error.

RFSs are well suited to represent any multi-target systems. However, they can be refined to better capture complex scenarios. In the next section, we derive a model for multi-group multi-target systems.

[1]If $m > n$, $\mathbf{X}$ and $\mathbf{Y}$ have to be switched.

3. MULTI-GROUP MULTI-OBJECT SYSTEMS

In this section, we first propose a hierarchical RFS model to represent a generic multi-group multi-target situation with coordinated-motion target groups. We then illustrate the applicability of this hierarchical model to different scenarios through two detailed examples. In a second sub-section, we propose a metric in order to quantify the difference between two hierarchical RFSs.

3.1. Proposed model: hierarchical RFS

A hierarchical RFS, illustrated by Fig. 1, is defined to represent the group and the target states. Let us first present the RFS at the group layer as follows:

$$\tilde{\mathbf{X}} = \left\{ \begin{bmatrix} \mathbf{X}_1 \\ \boldsymbol{\xi}_1 \end{bmatrix}, \begin{bmatrix} \mathbf{X}_2 \\ \boldsymbol{\xi}_2 \end{bmatrix}, ..., \begin{bmatrix} \mathbf{X}_{\tilde{m}} \\ \boldsymbol{\xi}_{\tilde{m}} \end{bmatrix} \right\}, \text{ with } \tilde{m} \in \mathbb{N}, \tag{6}$$

with $\tilde{m}$ the number of distinct groups, $\{\boldsymbol{\xi}_i\}_{i=1,...,\tilde{m}}$ the vector containing the group common parameters and $\{\mathbf{X}_i\}_{i=1,...,\tilde{m}}$ the RFS associated to the multi-target state conditionally defined to a specific group. Since $\boldsymbol{\xi}_i$ and $\mathbf{X}_i$ are random, the FISST PDF is similarly defined as in (2) and (3) by introducing the distribution on the group cardinality $\tilde{\rho}(\tilde{m})$ and the "spatial" symmetric distributions $r_{\tilde{m}}(.)$ in a FISST sense. It is defined as follows:

$$r_{\tilde{m}}\left(\begin{bmatrix} \mathbf{X}_1 \\ \boldsymbol{\xi}_1 \end{bmatrix}, ..., \begin{bmatrix} \mathbf{X}_{\tilde{m}} \\ \boldsymbol{\xi}_{\tilde{m}} \end{bmatrix} \right) = \prod_{i=1}^{\tilde{m}} f\left(\mathbf{X}_i|\boldsymbol{\xi}_i\right) p\left(\boldsymbol{\xi}_i\right), \tag{7}$$

with $f(.)$ a FISST PDF on the set $\mathbf{X}_i$ whereas $p(.)$ is a classical PDF. The state space is thus the cartesian product of the space of all multi-target RFSs and the space of the group common parameters. It should be noted that both $\mathbf{X}_i$ and $\boldsymbol{\xi}_i$ can be time varying. A time index k is added to account for it in the remainder of the paper when necessary.

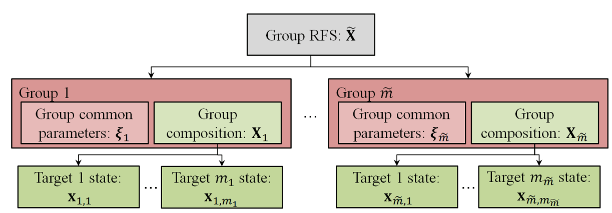

Fig. 1. Hierarchical RFS model.

At the target layer, a multi-target RFS $\mathbf{X}_i$ is conditionally defined to a group i and its vector of common parameters $\boldsymbol{\xi}_i$ as follows:

$$\mathbf{X}_i = \{\mathbf{x}_{i,1}, \mathbf{x}_{i,2}, ..., \mathbf{x}_{i,m_i}\}, \text{ with } m_i \in \mathbb{N}, \tag{8}$$

with $\{\mathbf{x}_{i,j}\}_{j=1,...,m_i}$ the target states gathering the kinematic parameters of a target such as its position, velocity and acceleration. The associated FISST PDF $f(.)$ on $\mathbf{X}_i$ is defined as in Eq. (2). In the next subsection, we illustrate the flexibility of our model by showing its applicability to different scenarios.

3.1.1. *First scenario: coordinated velocities*

In this scenario, all the targets in a given group have coordinated velocities. This means that the target velocities are mainly driven by the group motion but can differ slightly with one another due to the target own maneuvering capabilities. In the following 2D-plane example, the group i velocity is denoted $\tilde{\mathbf{v}}_{i,k} = [v_{i,k}^{(x)}, v_{i,k}^{(y)}]^T$. Thus, the common parameter $\boldsymbol{\xi}_{i,k}$ of the hierarchical RFS only includes $\tilde{\mathbf{v}}_{i,k}$. The deviation from the group velocity for the target j belonging to the group i is then denoted $\boldsymbol{\beta}_{i,j,k} = [\beta_{i,j,k}^{(x)}, \beta_{i,j,k}^{(y)}]^T$. Then, the time evolution of its state vector $\mathbf{x}_{i,j,k} = [x_{i,j,k}, \dot{x}_{i,j,k}, y_{i,j,k}, \dot{y}_{i,j,k}]^T$ for the x-coordinate is given by:

$$\begin{aligned} x_{i,j,k} &= x_{i,j,k-1} + (v_{i,k-1}^{(x)} + \beta_{i,j,k-1}^{(x)})T_s + u_{i,j,k}, \\ \dot{x}_{i,j,k} &= v_{i,k}^{(x)} + \beta_{i,j,k}^{(x)}, \end{aligned} \tag{9}$$

with T_s the sampling period whereas $u_{i,j,k}$ is a zero-mean Gaussian white sequence with variance $\sigma_{u_{i,j}}^2$. The velocity components have their own time evolutions generically defined as follows:

$$\begin{aligned} \beta_{i,j,k}^{(x)} &= g(\beta_{i,j,k}^{(x)}, w_{i,j,k}), \\ v_{i,k}^{(x)} &= h(v_{i,k-1}^{(x)}, q_{i,k}), \end{aligned} \tag{10}$$

with $g(.)$ and $h(.)$ the functions modeling the way the components of velocity are updated using respectively $w_{i,j,k}$ and $q_{i,k}$, two uncorrelated zero-mean Gaussian white sequences with variances $\sigma_{w_{i,j}}^2$ and $\sigma_{q_i}^2$. As usual in the RFS framework, a probability of birth and a probability to survive are defined to represent the possibility of a target to appear or disappear. In our approach, the same kind of probabilities are additionally defined at the group level. A realization of the scenario using the generative hierarchical RFS model is presented on Fig. 2.

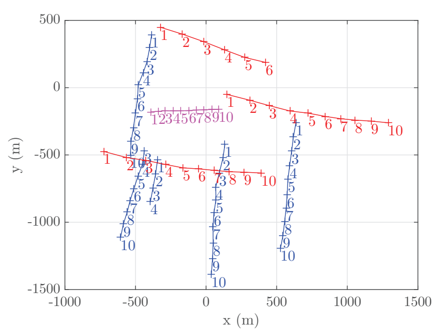

Fig. 2. One realization of the generative hierarchical model where a different color is used for each group and the target position is represented by a cross whose instant is indicated by the closest number.

3.1.2. *Second scenario: road constraints*

In [24], targets of a same group evolve along a section of a same road, in the same direction. It integrates road constraints by using curvilinear coordinates to define a target state $\mathbf{x}_k$ evolving on a particular road segment as follows:

$$\mathbf{x}_k \triangleq [l_k, \dot{l}_k]^T, \tag{11}$$

with l_k the arc length and $\dot{l}_k$ the associated speed. The road modeling is detailed in [25] and illustrated in Fig. 3.

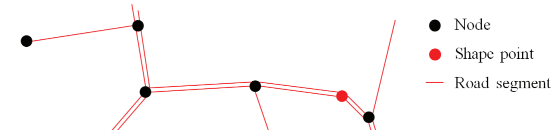

Fig. 3. Road segment model, with nodes modeling road intersections and shape points to follow road curvature.

In [24], to deal with motion dependencies of the vehicles, the authors propose to use a car-following model (CFM) based on a leading vehicle characterized by its state vector $\mathbf{x}_k^{(l)}$. The principle is to model the time evolution of the state vector $\mathbf{x}_k$ of a vehicle as follows:

$$\mathbf{x}_k = F_k \mathbf{x}_{k-1} + \Gamma_k \left(a_{k-1} + u_{k-1}\right), \tag{12}$$

with $F_k = \begin{bmatrix} 1 & T_s \\ 0 & 1 \end{bmatrix}$, $\Gamma_k = [T_s^2/2, T_s]^T$, T_s is the sampling period and u_{k-1} is a zero-mean Gaussian white noise sequence with variance $\sigma_{u_j}^2$. Moreover, a_{k-1} represents an acceleration induced by the traffic and its value depends on the state of the leading vehicle $\mathbf{x}_{k-1}^{(l)}$ as follows:

$$a_{k-1} = F_l \mathbf{x}_{k-1}^{(l)} + F_f \mathbf{x}_{k-1} + \rho, \tag{13}$$

where F_l, F_f and ρ are fixed parameters. See [26–29]. Note that Eq. (12) also holds for the leading vehicle by setting a_{k-1} to 0.

To address several target groups evolving simultaneously, the authors in [24] conduct clustering without using the RFS framework. Here, we show that this scenario can be fairly and easily represented by our hierarchical RFS model. For this purpose, the notations must be adjusted by introducing the additional subscripts. More particularly, i and j refer to the group and the target number respectively. In this case, the common parameter $\boldsymbol{\xi}_{i,k}$ of the group i includes the state of the leading vehicle $\mathbf{x}_{i,k-1}^{(l)}$ and the road segment identifier. The motion of the target associated to the state vector $\mathbf{x}_{i,j,k}$ is then described by (12) and (13).

In the next section, we propose a metric to compare two multi-target multi-group sets.

3.2. Proposed metric: multi-group OSPA (MG-OSPA)

3.2.1. *Definition of the metric*

Let us consider two multi-target multi-group sets defined as follows:

$$\tilde{\mathbf{X}} = \left\{ \begin{bmatrix} \mathbf{X}_1 \\ \boldsymbol{\xi}_1 \end{bmatrix}, ..., \begin{bmatrix} \mathbf{X}_{\tilde{m}} \\ \boldsymbol{\xi}_{\tilde{m}} \end{bmatrix} \right\} \text{ and } \tilde{\mathbf{Y}} = \left\{ \begin{bmatrix} \mathbf{Y}_1 \\ \boldsymbol{\kappa}_1 \end{bmatrix}, ..., \begin{bmatrix} \mathbf{Y}_{\tilde{n}} \\ \boldsymbol{\kappa}_{\tilde{n}} \end{bmatrix} \right\}, \tag{14}$$

with $(\tilde{m}, \tilde{n}) \in \mathbb{N}^2$. The two hierarchical RFSs $\tilde{\mathbf{X}}$ and $\tilde{\mathbf{Y}}$ may differ in the number of groups, in the assignment of the targets to the groups but also at the group level, in the group parameter vectors and in the group conditional multi-target RFSs. Therefore, we propose the following metric between these two sets when[2] $\tilde{m} \leq \tilde{n}$:

$$\tilde{d}_r^{(\tilde{c})}\!\left(\tilde{\mathbf{X}},\tilde{\mathbf{Y}}\right) = \left(\frac{1}{\tilde{n}}\left(\min_{\tilde{\pi}\in\Pi_{\tilde{n}}} \sum_{\tilde{i}=1}^{\tilde{m}} \left[\tilde{d}_{\tilde{c}}^{q}\!\left(\begin{bmatrix} \mathbf{X}_{\tilde{i}} \\ \boldsymbol{\xi}_{\tilde{i}} \end{bmatrix}, \begin{bmatrix} \mathbf{Y}_{\tilde{\pi}(\tilde{i})} \\ \boldsymbol{\kappa}_{\tilde{\pi}(\tilde{i})} \end{bmatrix}\right)\right]^r + \tilde{c}^r(\tilde{n}-\tilde{m})\right)\right)^{\frac{1}{r}}, \tag{15}$$

with $\tilde{c}$ the cut-off parameter of the multi-target multi-group metric, r the order, $\Pi_{\tilde{n}}$ the set of permutations on $\{1, 2, ..., \tilde{n}\}$ and $\tilde{d}_{\tilde{c}}^q(.)$ the metric between two extended multi-target sets defined as follows:

$$\tilde{d}_{\tilde{c}}^{q}\!\left(\begin{bmatrix} \mathbf{X} \\ \boldsymbol{\xi} \end{bmatrix}, \begin{bmatrix} \mathbf{Y} \\ \boldsymbol{\kappa} \end{bmatrix}\right) = \min\left(\tilde{c}, \left[\left(d_p^{(c)}\left(\mathbf{X}, \mathbf{Y}\right)\right)^q + \left(\gamma d_g\left(\boldsymbol{\xi}, \boldsymbol{\kappa}\right)\right)^q\right]^{\frac{1}{q}}\right), \tag{16}$$

[2] If $\tilde{m} > \tilde{n}$, $\tilde{\mathbf{X}}$ and $\tilde{\mathbf{Y}}$ have to be switched.

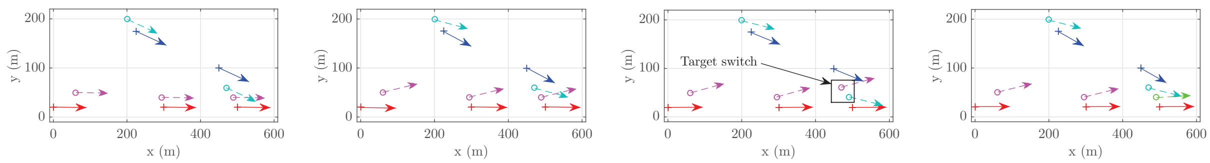

(a) (b) (c) (d)

Fig. 4. Four examples of multi-target multi-group realizations. Targets of a same group share the same color. Arrows represent the group velocities associated to each target. The first hierarchical RFS contains red and blue targets while the second one contains the magenta and the cyan targets (and also the green in (d)).

where $d_p^{(c)}(.)$ is the OSPA metric as defined in (4), q is the order whereas $d_g(.)$ is the Euclidean metric between the parameter vectors $\boldsymbol{\xi}$ and $\boldsymbol{\kappa}$ of the two compared groups. In addition, γ is a scaling parameter so that $\gamma d_g(.)$ is in the interval $[0, c]$. The metric proposed in (15) is built similarly to the OSPA. $\tilde{d}_r^{(\tilde{c})}(\tilde{\mathbf{X}}, \tilde{\mathbf{Y}})$ aims at taking into account different features: the errors made on the group number through the quantity $\tilde{c}^r\,(\tilde{n} - \tilde{m})$, the error made on the group parameters through $\gamma d_g\,(\boldsymbol{\xi}, \boldsymbol{\kappa})$ in (16), the errors made on the states and the group compositions through $d_p^{(c)}\,(\mathbf{X}, \mathbf{Y})$ in (16). The higher the orders p, q and r are, the more penalized high values of their corresponding metrics are. Similarly to the setting of the value of c, $\tilde{c}$ represents the maximum value of the metric. Note that the cardinality and assignment errors are dimensionless while the group and individual state parameters are not necessarily expressed in the same units. The scaling parameter γ ensures that the formula remains homogeneous and makes the balance between the different sources of errors.

Finally, since the structure of the proposed distance is inherited from the OSPA one, the Hungarian method [30] can be used to make the computation efficient. Also, variants similar to that of the OSPA can be considered.

3.2.2. *Proof: MG-OSPA is a metric*

In (15), $\tilde{d}_r^{(\tilde{c})}(.,.)$ takes the form of the classical OSPA metric [8]. According to [8], it is a metric if $\tilde{d}_{\tilde{c}}^q(.,.)$ defined in (16) is a metric with values in $[0, \tilde{c}]$. Elements of proof are given below:

1) the range of $\tilde{d}_{\tilde{c}}^q(.,.)$ is $[0, \tilde{c}]$ by definition (15).

2) $\tilde{d}_{\tilde{c}}^q(.,.)$ is a metric if $[(d_p^{(c)}(.,.))^q + (\gamma d_g(.,.))^q]^{\frac{1}{q}}$ is a metric. As $d_p^{(c)}(.,.)$ and $d_g(.,.)$ are two metrics defined on their respective spaces, $q \in [1, +\infty]$ and $\gamma > 0$, the non-negativity, the identity of indiscernibles and the symmetry are inherited properties. Let us consider three extended sets $\begin{bmatrix}\mathbf{X}\\ \boldsymbol{\xi}\end{bmatrix}$, $\begin{bmatrix}\mathbf{Y}\\ \boldsymbol{\kappa}\end{bmatrix}$ and $\begin{bmatrix}\mathbf{Z}\\ \boldsymbol{\zeta}\end{bmatrix}$, by taking advantage of the triangle inequality on $d_p^{(c)}(\mathbf{X}, \mathbf{Y})$ and $d_g(\boldsymbol{\xi}, \boldsymbol{\kappa})$, one has:

$$\begin{aligned}&[(d_p^{(c)}(\mathbf{X}, \mathbf{Z}))^q + (\gamma d_g(\boldsymbol{\xi}, \boldsymbol{\zeta}))^q]^{\frac{1}{q}} \qquad (17)\\ &\leq [(d_p^{(c)}(\mathbf{X}, \mathbf{Y}) + d_p^{(c)}(\mathbf{Y}, \mathbf{Z}))^q + (\gamma d_g(\boldsymbol{\xi}, \boldsymbol{\kappa}) + \gamma d_g(\boldsymbol{\kappa}, \boldsymbol{\zeta}))^q]^{\frac{1}{q}}.\end{aligned}$$

Given the above equation, the Minkowski inequality makes it possible to conclude that:

$$\begin{aligned}&[(d_p^{(c)}(\mathbf{X}, \mathbf{Y}) + d_p^{(c)}(\mathbf{Y}, \mathbf{Z}))^q + (\gamma d_g(\boldsymbol{\xi}, \boldsymbol{\kappa}) + \gamma d_g(\boldsymbol{\kappa}, \boldsymbol{\zeta}))^q]^{\frac{1}{q}}\\ &\qquad \leq [(d_p^{(c)}(\mathbf{X}, \mathbf{Y}))^q + (\gamma d_g(\boldsymbol{\xi}, \boldsymbol{\kappa}))^q]^{\frac{1}{q}} \qquad (18)\\ &\qquad + [(d_p^{(c)}(\mathbf{Y}, \mathbf{Z}))^q + (\gamma d_g(\boldsymbol{\kappa}, \boldsymbol{\zeta}))^q]^{\frac{1}{q}}.\end{aligned}$$

Thus, $[(d_p^{(c)}(.,.))^q + (\gamma d_g(.,.))^q]^{\frac{1}{q}}$ is a metric and consequently $\tilde{d}_{\tilde{c}}^q(.,.)$ too. Given 1) and 2), $\tilde{d}_r^{(\tilde{c})}(.,.)$ is a metric.

3.2.3. *Examples*

In this section, we present a set of examples to compare the behaviors of the OSPA and the MG-OSPA for hierarchical RFSs built with coordinated velocities. Situations are represented on the Fig. 4 (a), (b), (c) and (d) where there are five targets. Three of them belong to a group whereas the two others belong to another group. The values of OSPA and MG-OSPA are given in table 1, with $\gamma = 1$, $c = 100$, $\tilde{c} = 200$, $p = 1$, $q = 1$ and $r = 1$.

In Fig. 4 (a), we consider the situation where the positions differ between the two compared RFSs whereas the clustering and the velocities are identical. The MG-OSPA is greater than the OSPA because it computes an OSPA for each group. In Fig. 4 (b), not only the positions differ, but also the group velocities. It illustrates how the MG-OSPA evolves when the errors on the group parameters grow. In Fig. 4 (c) and 4 (d), errors at the group level are considered. In the first case, the number of groups is the same but the targets are allocated differently whereas in the second case, one of the target forms an additional group. In both cases, the OSPA does not account for such errors while the MG-OSPA is increased. The behavior of the proposed metric is confirmed by the results presented in table 1. They show that it is able to quantify the errors on positions, velocities and group assignments in a multi-target scenarios. Note also that analyzing separately the different terms of the MG-OSPA makes it possible to identify the source of error, *e.g.* different positions and velocities or clustering issues.

Scenarios	Fig. 4 (a)	Fig. 4 (b)	Fig. 4 (c)	Fig. 4 (d)
OSPA	42.14	42.14	42.14	42.14
MG-OSPA	43.50	50.01	61.47	268.41

Table 1. Values of OSPA and MG-OSPA depending on situations represented on Fig. 4.

4. CONCLUSION AND PERSPECTIVES

In this paper, a new model based on a hierarchical RFS is presented for multi-target multi-group scenarios. A first RFS is intuitively used for the groups whose number, common characteristics and compositions are evolving parameters. The composition of a group is then itself represented by an RFS to model the variable number of targets inside the group and their states. Two types of scenarios are detailed in the paper to illustrate the relevance of the proposed model. By taking advantage of the OSPA formulation, we also derive a metric for this hierarchical RFS and show how it can be used complementary to the classical OSPA. Based on this hierarchical model, we are currently developing an estimator for multi-target multi-group situations. We are considering the combination of a LMB filter to estimate the group RFS whereas a PHD is launched at the target layer.

5. REFERENCES

[1] D. Daley and D. Vere-Jones, *An introduction to the theory of point processes*, Springer, New-York, 1988.

[2] R. Mahler, “Multitarget Bayes filtering via first-order multitarget moments,” *IEEE Trans. on Aerospace and Electronic Systems*, vol. 39, no. 4, pp. 1152–1178, 2003.

[3] R. Mahler, *Statistical multisource-multitarget information fusion*, Artech House Inc., Norwood, 2007.

[4] S. Reuter, B.-T. Vo, B.-N. Vo, and K. Dietmayer, “The labeled multi-Bernoulli filter,” *IEEE Trans. on Signal Processing*, vol. 62, no. 12, pp. 3246–3260, 2014.

[5] B.-T. Vo and B.-N. Vo, “Labeled random finite sets and multi-object conjugate priors,” *IEEE Trans. on Signal Processing*, vol. 61, no. 13, pp. 3460–3475, 2013.

[6] R. T. Rockafellar and R. J.-B. Wets, *Variational analysis*, Springer Verlag, 1998.

[7] J. Hoffman and R. Mahler, “Multitarget miss distance via optimal assignment,” *IEEE Trans. on Systems, Man, and Cybernetics*, vol. 34, no. 3, pp. 327–336, 2004.

[8] D. Schuhmacher, B.-T. Vo, and B.-N. Vo, “A consistent metric for performance evaluation of multi-object filters,” *IEEE Trans. on Signal Processing*, vol. 56, no. 8, pp. 3447–3457, 2008.

[9] S. Nagappa, D. E. Clark, and R. Mahler, “Incorporating track uncertainty into the OSPA metric,” *14th Conference on Information Fusion*, pp. 1–8, 2011.

[10] X. He, R. Tharmarasa, T. Kirubarajan, and T. Thayaparan, “A track quality based metric for evaluating performance of multitarget filters,” *IEEE Trans. on Aerospace and Electronic Systems*, vol. 49, no. 49, pp. 610–616, 2013.

[11] A. S. Rahmathullah, Á. F. García-Fernández, and L. Svensson, “Generalized optimal sub-pattern assignment metric,” *20th Conference on Information Fusion*, pp. 1–8, 2017.

[12] X. Shi, F. Yang, F. Tong, and H. Lian, “A comprehensive performance metric for evaluation of multi-target tracking algorithms,” *3rd Int. Conference on Information Management*, pp. 373–377, 2017.

[13] B. Ristic, B.-N. Vo, and D. Clark, “Performance evaluation of multi-target tracking using the OSPA metric,” *13th Conference on Information Fusion*, pp. 1–7, 2010.

[14] B. Ristic, B.-N. Vo, D. Clark, and B.-T. Vo, “A metric for performance evaluation of multi-target tracking algorithms,” *IEEE Trans. on Signal Processing*, vol. 59, no. 7, pp. 3452–3457, 2011.

[15] P. Barrios, G. Naqvi, M. Adams, K. Leung, and F. Inostroza, “The cardinalized optimal linear assignment (COLA) metric for multi-object error evaluation,” *18th Conference on Information Fusion*, pp. 271–279, 2015.

[16] Z. Shujun, L. Weifeng, W. Chenglin, and C. Hailong, “Multiple group targets tracking using the generalized labeled multi-Bernoulli filter,” *35th Chinese Control Conference*, pp. 4871–4876, 2016.

[17] W. Koch, “Bayesian approach to extended object and cluster tracking using random matrices,” *IEEE Trans. on Aerospace and Electronic Systems*, vol. 44, no. 3, pp. 1042–1059, 2008.

[18] K. Gilholm and D. Salmond, “Spatial distribution model for tracking extended objects,” *IEE Radar, Sonar and Navigation*, vol. 152, no. 5, pp. 364–371, 2005.

[19] R. Mahler, “PHD filters for nonstandard targets, I: Extended targets,” *Int. Conference on Information Fusion*, pp. 915–921, 2009.

[20] D. Schuhmacher and A. Xia, “A new metric between distributions of point processes,” *Advances in Applied Probability*, vol. 40, no. 3, pp. 651–672, 2008.

[21] C. Magnant, A. Giremus, E. Grivel, L. Ratton, and B. Joseph, “Multi-target tracking using a PHD-based joint tracking and classification algorithm,” *IEEE Radar Conference*, pp. 1–6, 2016.

[22] M. Guerriero, L. Svensson, D. Svensson, and P. Willett, “Shooting two birds with two bullets: how to find minimum mean OSPA estimates,” *13th Conference on Information Fusion*, pp. 1–8, 2010.

[23] M. Baum, B. Balasingam, P. Willett, and U. Hanebeck, “OSPA barycenters for clustering set-valued data,” *18th Conference on Information Fusion*, pp. 1375–1381, 2015.

[24] D. Song, R. Tharmarasa, T. Kirubarajan, and X. N. Fernando, “Multi-vehicle tracking with road maps and car-following models,” *IEEE Trans. on Intelligent Transportation Systems*, vol. no. 99, pp. 1–12, 2017.

[25] D. Betaille and R. Toledo-Moreo, “Creating enhanced maps for lane-level vehicle navigation,” *IEEE Trans. on Intelligent Transportation Systems*, vol. 11, no. 4, pp. 786–798, 2010.

[26] W. Helly, “Simulation of bottlenecks in single lane traffic flow,” *Proc. Theory Traffic Flow*, pp. 207–238, 1959.

[27] T. H. Rockwell, R. L. Ernst, and A. Hanken, “A sensitivity analysis of empirically derived car-following models,” *Transp. Res.*, vol. 2, no. 4, pp. 363–373, 1968.

[28] G. A. Bekey, G. O. Burnham, and J. Seo, “Control theoretic models of human drivers in car following,” *Human Factors, J. Human Factors Ergonom. Soc.*, vol. 19, no. 4, pp. 399–413, 1977.

[29] M. Aron, “Car following in an urban network: Simulation and experiments,” *Planning Transp. Res. Comput.*, vol. 46, no. 8, pp. 27–39, 1988.

[30] H. W. Kuhn, “The Hungarian method for the assignment problem,” *Naval Research Logistics Quarterly*, vol. 2, pp. 83–97, 1955.